Int. J. Nano Dimens., 11 (4): 392-398, Autumn 2020

ORIGINAL ARTICLE

Computational study of bandgap-engineered Graphene nano ribbon tunneling field effect transistor (BE-GNR-TFET)

Soheil Abbaszadeh, Seyed Saleh Ghoreishi*, Reza Yousefi, Habib Aderang

Department of Electrical Engineering, Nour Branch, Islamic Azad University, Nour, Iran

Received 08 April 2020; revised 06 June 2020; accepted 08 June 2020; available online 15 August 2020

Abstract

By applying tensile local uniaxial strain on 5 nm of drain region and compressive local uniaxial strain on 2.5 nm of source and 2.5 nm of channel regions of graphene nanoribbon tunneling field-effect transistor (GNR-TFET), we propose a new bandgap-engineered (BE) GNR-TFET. Simulation of the suggested device is done based on non-equilibrium Green's function (NEGF) method by a mode-space approach. Simulation results show that, compared to the conventional GNR-TFET, the BE-GNR-TFET enjoys from a better am-bipolar behavior and a higher on-current. Besides, the analog characteristic of the proposed structure such as transconductance (g_m) and unity-gain frequency (f_t) is also improved.

Keywords: *Density of States (DOS); Graphene Nanoribbon (GNR); Non-Equilibrium Green's Function (NEGF); Tunneling Field Effect; Unity Gain Frequency (ft).*

How to cite this article

Abbaszadeh S., Ghoreishi SS., Yousefi R., Habib Aderang. Computational study of bandgap-engineered Graphene nano ribbon tunneling field effect transistor (BE-GNR-TFET) . Int. J. Nano Dimens., 2020; 11 (4): 392-398.

INTRODUCTION

In recent years, reducing the size of the common CMOS transistors to less than 100 nm for gaining a higher integration density and a higher speed has faced multiple problems including, an increase in the static power consumption caused by an increase in three parameters of the am-bipolar current, the sub-threshold-swing and the leakage current [1-2].

In order to improve the energy efficiency of the electronic circuits, tunneling field effect transistors have been introduced [3-4]. Tunnel FETs have a P-I-N structure and their on-current is of the band to band tunneling (BTBT) type. Because of the current mechanism, they have a very low subthreshold slope and are therefore well suited for low-power applications [5-6].

Graphene and graphene nanoribbons have unique and highly promising properties, such as direct energy-bandgap, very small width, and at the same time, high strength and high electron mobility. These materials have nowadays attracted a lot of attention and are utilized at the channel of field effect transistors [7-8].

In order to enhance the electric properties of GNR-based TFETs, different techniques have already been adopted such as dual material gate [9-11], hetero-structure chirality [12], electrically activation or charge plasma [13-15], and lightly doped source and drain [12-16]. In most studies, it was mainly aimed to reduce the am-bipolar current, which sometimes leading to the reduction of the on-current.

The present study has investigated the possibility of simultaneously improving the on-current and am-bipolar current of a GNR-based TFET by applying a compressive and tensile local strain to the source-channel and channel-drain regions, respectively. It is also worth noting that, GNR is about an atomic layer in thickness, which allows for the exertion of local strain on it by placing graphene over a sub-layer or oxide-fabricated

* Corresponding Author Email: salehghoreyshi@gmail.com

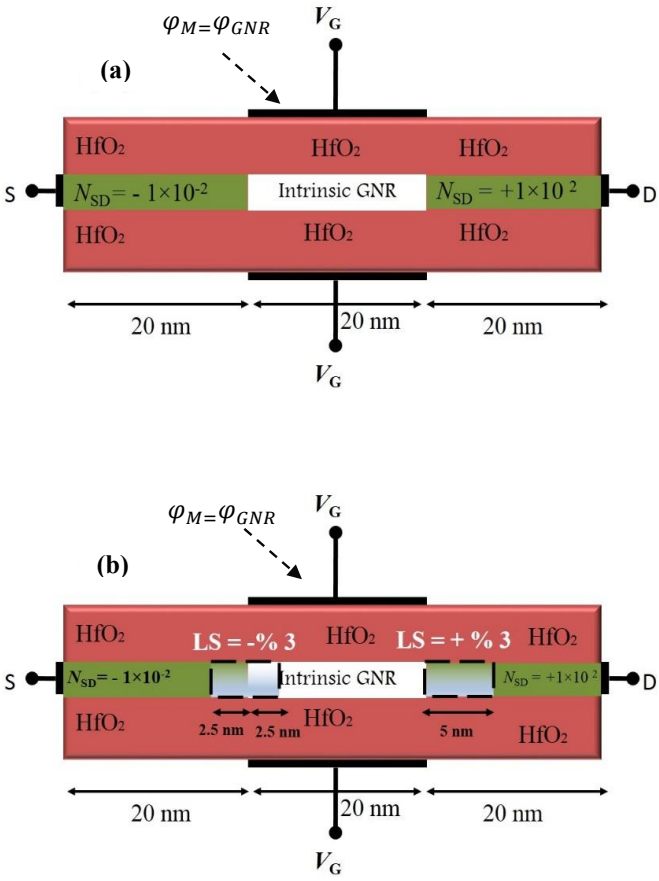

Fig. 1. Schematic cross-sectional of the (a) conventional TFET and (b) proposed structure.

patterned like trenches [17-18]. The rest of the paper is organized as follows: in Device structure and Simulation method section, the modified and the conventional structure are introduced and the simulation method will be explained. The simulation results will be discussed in the Results and Discussion section, followed by a conclusion of the study in the last section.

Device Structure and simulation method

As explained before, tunneling transistors suffer from a low on-current and an inappropriate am-bipolar behavior. The on-current and am-bipolar behavior in the tunneling structure are caused respectively by the carriers' tunneling from the valence band of the source to the conduction band of the channel and the carriers' tunneling from the channel valence band to the drain conduction band. By increasing the tunneling barrier width on the channel-drain side, the am-bipolar current has been reduced, while by decreasing the tunneling width on the source-channel side, the on-current has been increased. To this end, this study has thus applied the local strain onto the suggested structure.

Figs. 1 (a) and (b) show the conventional GNR-TFET and the bandgap engineered (BE) GNR-TFET, respectively. The length of structure is considered to be 60 nm, and each of the source, channel, and drain regions is supposed to be 20 nm. The considered oxide is HfO_2 having a dielectric constant of 16 (K = 16) with the thickness of 2 nm. The channel material is GNR of the type armchair with n=12 and the doping densities of the source and drain regions are of the type *P*+ and *N*+, respectively, with N_{SD}=10^{-2} dopants per atom. The work function of gate materials ($\ddot{O}_M$) is chosen to be similar to that of the graphene nanoribbon ($\ddot{O}_{GNR}$). In the proposed structure, in order to increase the on-current and decrease the off-current and am-bipolar behavior, local strain is applied onto the source-channel and channel-

drain regions, respectively. Bandgap engineering (BE) of the proposed structure has been done by applying local uniaxial strain. As shown in the figure, a compressive local strain of -%3 is applied to 5 nm of source and channel (2.5 nm of the source and 2.5 nm of the channel) in order to increase the on-current; moreover, a tensile local strain of +%3 is applied to 5 nm of the drain in order to decrease the am-bipolar and leakage current.

To obtain the characteristics of the modified structure, the Poisson and the Schrödinger equations have been solved simultaneously in a self-consistent manner using the non-equilibrium Green's function (NEGF) method by the mode-space approach. Potential distribution given by the Poisson equation is used at the Green's function by the following equation [19-20]:

$$G=\left[(E+i0^{+})I-H-\Sigma\right]^{-1}\approx\left[EI-H-\Sigma\right]^{-1} \quad (1)$$

where, *E*, 0^{+} and I are energy, a positive infinitesimal number and the identity matrix. H is the Hamiltonian matrix and $\sum_{S(D)}$ is the source (drain) self-energy matrix. Hamiltonian matrix of q^{th} mode is computed as follows:

$$H=\begin{bmatrix} U_1 & \mathrm{b}_{2q} & 0 & t_3 & & \\ \mathrm{b}_{2q} & U_2 & \mathrm{b}_{1q} & 0 & \ddots & \\ 0 & \mathrm{b}_{1q} & \mathrm{U}_3 & \mathrm{b}_{2q} & 0 & t_3 \\ t_3 & 0 & \mathrm{b}_{2q} & \ddots & \ddots & \ddots \\ & \ddots & 0 & \ddots & \ddots & \ddots \\ & & t_3 & \ddots & \ddots & \mathrm{U}_M \end{bmatrix} \quad (2)$$

Where, U_i, t_3, b_{2q} and b_{1q} are the on-site electrostatic potential at the *i*-th GNR ring, the hopping parameters between the third, second and first nearest-neighbor GNR rings for the *q*-th mode, respectively, which have been computed as follows [21]:

$$\mathrm{b}_{1q}=t_0\left(1+4C_{edge}sin^2\left(\pi q/(n+1)\right)/(n+1)\right) \quad (3\text{-a})$$

$$\mathrm{b}_{2q}=2t_0\cos\left(\pi q/(n+1)\right) \quad (3\text{-b})$$

$$t_3\approx 0.2eV \quad (3\text{-c})$$

$t_0\approx 2.7eV$ is the tight-binding parameter between two nearest-neighbor carbon atom and $C_{edge}=0.12$ is the edge bond relaxation parameter. When the uniaxial strain is applies to the GNR, some elements of the Hamiltonian matrix should be changed by the Harrison relation as follows [22]:

$$b_{1q(new)}=b_{1q(old)}\left(1+\frac{\Delta l}{l}\right)^2 \quad (4\text{-a})$$

$$b_{2q(new)}=2t\left[1+\frac{\Delta l}{2l}\right]cos\left(\frac{\pi q}{n}\right) \quad (4\text{-b})$$

where l is the nanoribbon length before strain and Δl is the nanoribbon length variation after deformation. Further details of the simulation method have been described in the previous works [23, 24].

RESULTS AND DISCUSSION

The effect of strain on the electronic properties of nanoribbon is heavily dependent on its edge shape and chirality. For an armchair graphene nanoribbon, we used a very small or large amount of uniaxial strain results in linear or periodic changes of the energy bandgap. As shown in Fig. 2, the energy bandgap in graphene nanoribbon with a chirality of *n*=12 in terms of uniaxial strain ranging from -%6 to +%6 increases linearly. To achieve the best value of local strain in our suggested structure, three values of %1, %3, and %5 have been investigated for the compressive and tensile local strain. In this context, the best value of local strain is observed to be %3, where the energy bandgap is changed by around %50.

Fig. 3 compares the I_{DS}-V_{GS} characteristic of the conventional TFET with that of local-strained structure. According to this figure, the proposed structure outperforms the conventional one by having a lower am-bipolar current and a higher on-current. Moreover, from this figure, it can be realized that the local-strained structure has a better subthreshold-swing.

To justify the am-bipolar behavior, the diagrams of the electron density spectrum for different energy levels along the device at V_{GS}=-0.2 V and V_{DS}=0.4 V have been depicted for the conventional structure and the proposed structure in Figs. 4 (a) and (b), respectively. As shown in these figures, by applying tensile local strain onto a part of the drain side, the energy bandgap, and as a result, the tunneling barrier width on the drain side increases, and so the am-bipolar current decreases. Since the off-current occurs due to the tunneling of the carriers from the channel valence band to the drain conduction band, using of local compressive uniaxial strain on the source and channel regions, have a negligible effect on the am-bipolar and off-current.

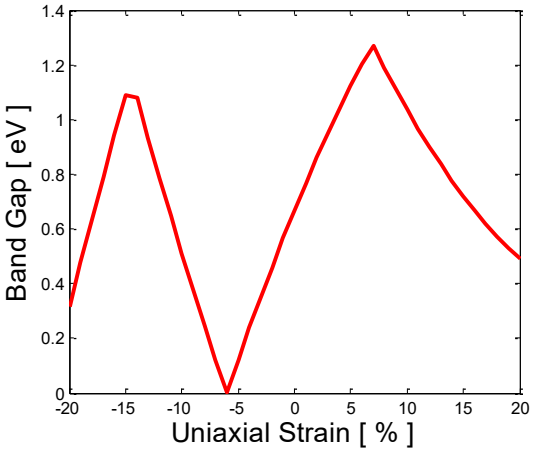

Fig. 2. Bandgap variation in terms of uniaxial strain.

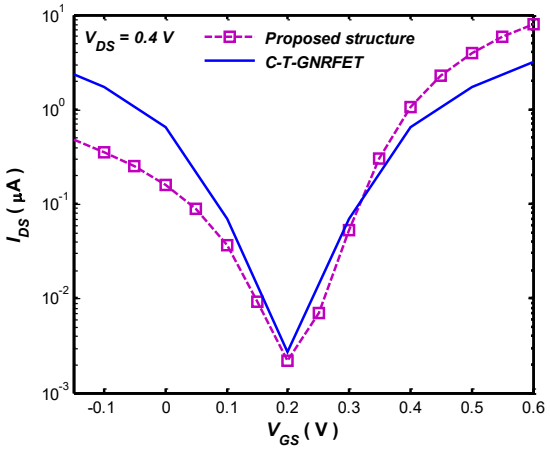

Fig. 3. Comparison of the I_{DS}-V_{GS} characteristic of the proposed structure (dashed line with symbol) and conventional T-GNRFET (line) at V_{DS}=0.4 V.

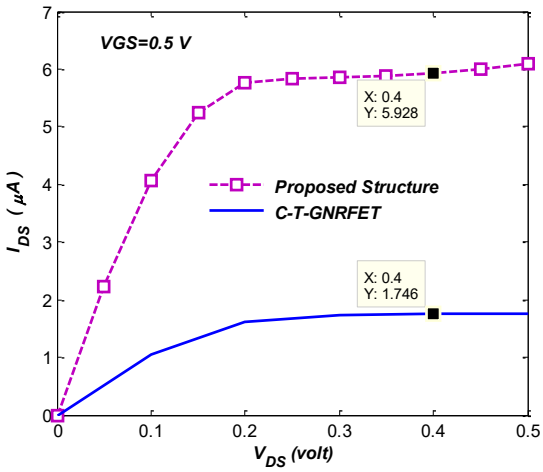

Fig. 4. Energy band diagrams (white lines) and the electron density spectrum across the (a) C-T-GNRFET and (b) proposed structure at V_{GS}=-0.2 V and V_{DS}=0.4 V.

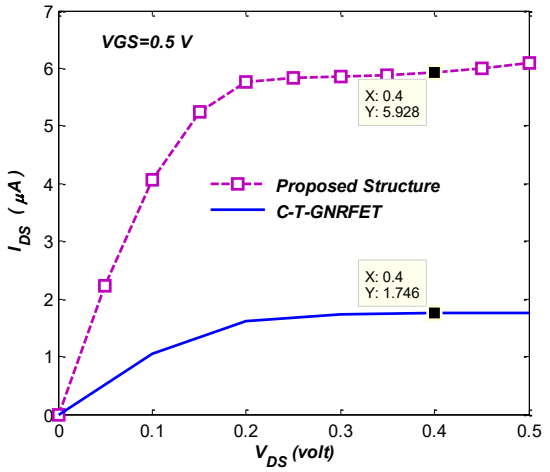

Fig. 5. I_{DS}-V_{DS} characteristic of the local-strained TFET (dashed line with symbol) and C-T-GNRFET (line) at V_{GS}=0.5 V.

Fig. 5 represents the I_{DS}-V_{DS} characteristic of the common TFET and that of the local-strained TFET at V_{GS}=0.5 V. The on-current in the proposed structure increases considerably. For example, as this figure shows, at V_{DS}=0.4 V and V_{GS}=0.5 V, the on-current increases from 1.74 mA (of the common structure) to 5.92 mA (in our suggested structure).

The diagrams of the electron density spectrum along the device in the on-state and for V_{GS}=0.5 V and V_{DS}=0.4 V have been illustrated in Fig. 6 (a) and (b), respectively. Due to the application of the compressive local strain to 2.5 nm of the channel and to 2.5 nm of the source, the energy bandgap and the tunneling width reduce in these regions, and hence the on-current increases.

Fig. 7 shows the comparison of transconductance (g_m) changes in terms of the gate-source voltage variations. Compared to the conventional structure, the proposed structure has a higher g_m, which can be explained by the increased sensitivity of the current to the gate-source voltage variations. Applying local strain on the source side leads to the reduction of the tunneling width. Due to the tunneling nature of the current, the current exponentially increases as the tunneling width decreases. The following formula is used to calculate g_m: $g_m = \frac{\partial I_{DS}}{\partial V_{GS}}$.

Next, the changes of the unity gain

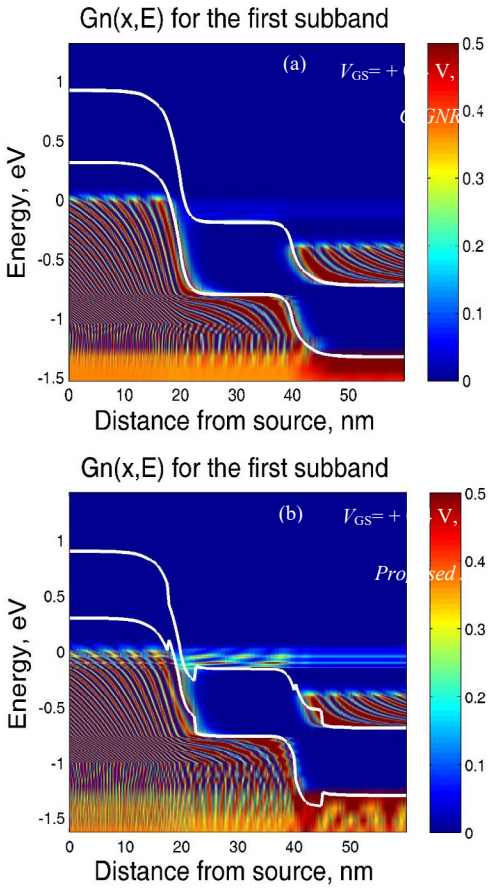

Fig. 6. Energy band diagrams (white lines) and the electron density spectrum across the (a) C-T-GNRFET and (b) proposed structure at V_{GS}=0.4 V and V_{DS}=0.4 V.

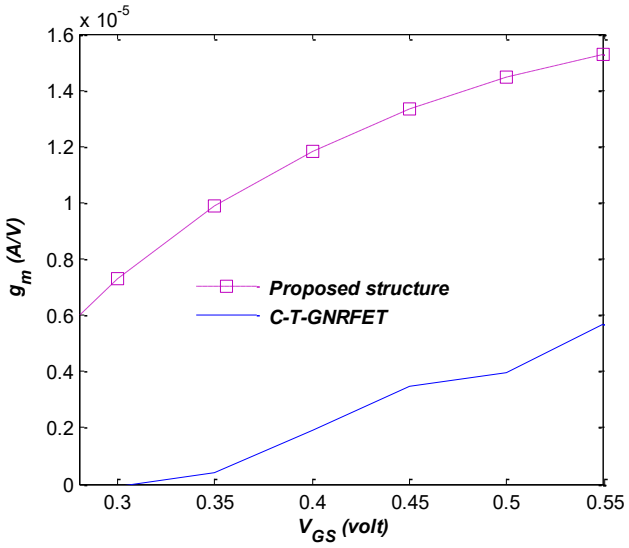

Fig. 7. The gate transconductance (g_m) of the local-strained T-GNRFET with those of conventional one vs gate-source voltage biased at V_{DS}=0.4 V.

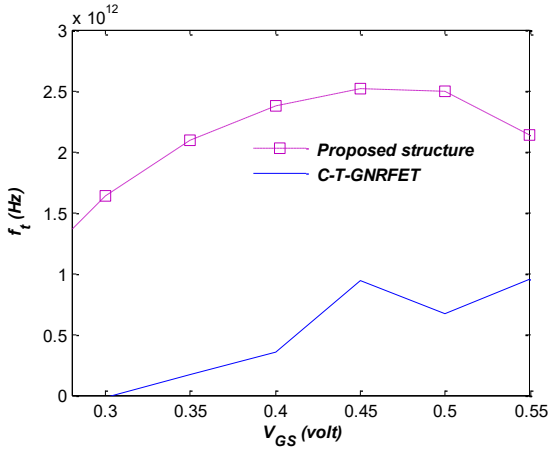

Fig. 8. Comparison of the unity gain frequency of the proposed structure (dashed line with symbol) and conventional T-GNRFET (line) at V_{DS}=0.4 V.

frequency () for the gate-source voltage variations has been shown and compared in Fig. 8. f_t has been calculated as follows: $f_t = \frac{g_m}{2\pi C_g}$.

Based on the above formula, f_t depends on two parameters of g_m and gate capacitor (*C*g). *C*g is the series combination of oxide capacitance (*C*ox) and quantum capacitance (C_Q). *C*ox is equal in the two structures owing to their similar gate structures. However, in the proposed structure, by applying local strain into the considered parts, the C_Q and thus the *C*g will increase. Since, in our proposed structure, g_m has increased more than C_Q, the f_t will also increase.

CONCLUSION

In the present study, by applying local uniaxial strain on 2.5 nm of source and channel and 5 nm of drain region, we have introduced a modified T-GNRFET. Simulations show that the proposed device exhibits on-current up to about 2.5 order of magnitude larger than that of its conventional rival. Furthermore, analog characteristics of the device such as transconductance and unity-gain frequency have also been shown to be superior to that of the conventional TFET. For the simulation, we employed non-equilibrium Green's function (NEGF) method by the mode-space transformation.

CONFLICTS OF INTEREST

The authors do not have any personal or financial conflicts of interest.

REFERENCES

[1] Arden W. M., (2002), The international technology roadmap for semiconductors—perspectives and challenges for the next 15 years. *Current Opin. Solid State and Mater. Sci.* 6: 371-377.

[2] Zhao H., Chen Y., Wang Y., Zhou F., Xue F., Lee J., (2011), InGaAs tunneling field-effect-transistors with atomic-layer-deposited gate oxides. *IEEE Transact. Elect. Dev.* 58: 2990-2995.

[3] Ionescu A. M., Riel H., (2011), Tunnel field-effect transistors as energy-efficient electronic switches. *Nature*. 479: 329-337.

[4] Seabaugh A. C., Zhang Q., (2010), Low-voltage tunnel transistors for beyond CMOS logic. *Proceed. IEEE*. 98: 2095-2110.

[5] Lv Y., Qin W., Wang C., Liao L., Liu X., (2019), Recent advances in low-dimensional heterojunction-based tunnel field effect transistors. *Adv. Electron. Mater.* 5: 1800569-1800573.

[6] Kim S., Luisier M., Boykin T. B., Klimeck G., (2014), Computational study of heterojunction graphene nanoribbon tunneling transistors with pd orbital tight-binding method. *Appl. Phys. Lett.* 104: 243113-243119.

[7] Celis A., Nair M. N., Taleb-Ibrahimi A., Conrad E. H., Berger C., De Heer W. A., Tejeda A., (2016), Graphene nanoribbons: fabrication, properties and devices. *J. Phys. D: Appl. Phys.* 49: 143001-143007.

[8] Gunlycke D., White C. T., (2008), Tight-binding energy dispersions of armchair-edge graphene nanostrips. *Phys. Rev. B*. 77: 115116-115121.

[9] Ghoreishi S. S., Saghafi K., Yousefi R., Moravvej-Farshi M. K., (2016), A novel tunneling graphene nano ribbon field effect transistor with dual material gate: Numerical studies. *Superlatt. Microstruct.* 97: 277-286.

[10] Naderi A., (2015), Theoretical analysis of a novel dual gate metal–graphene nanoribbon field effect transistor. *Mater. Sci. Semiconduc. Process.* 31: 223-228.

[11] Faraji M., Ghoreishi S. S., Yousefi R., (2018), Gate structural engineering of MOS-like junctionless Carbon nanotube

field effect transistor (MOS-like J-CNTFET). *Int. J. Nano Dimens.* 9: 32-40.

[12] Ghoreishi S. S., Saghafi K., Yousefi R., Moravvej-Farshi M. K., (2014), Graphene nanoribbon tunnel field effect transistor with lightly doped drain: Numerical simulations. *Superlatt. Microstruc.* 75: 245-256.

[13] Tahaei S. H., Ghoreishi S. S., Yousefi R., Aderang H., (2019), A computational study of a carbon nanotube junctionless tunneling field-effect transistor (CNT-JLTFET) based on the charge plasma concept. *Superlatt. Microstruct.* 125: 168-176.

[14] Ghoreishi S. S., Yousefi R., Taghavi, N., (2017), Performance evaluation and design considerations of electrically activated drain extension tunneling GNRFET: A quantum simulation study. *J. Electronic. Mater.* 46: 6508-6517.

[15] Tamersit K., (2019), A new ultra-scaled graphene nanoribbon junctionless tunneling field-effect transistor: Proposal, quantum simulation, and analysis. *J. Comput. Electron.* 1-7.

[16] Yousefi R., Saghafi K., Moravvej-Farshi M. K., (2010), Numerical study of lightly doped drain and source carbon nanotube field effect transistors. *IEEE Transact. Electron Dev.* 57: 765-771.

[17] Lee C., Wei X., Kysar J. W., Hone J., (2008), Measurement of the elastic properties and intrinsic strength of monolayer graphene. *Science*. 321: 385-388.

[18] Guinea F., Katsnelson M. I., Geim A. K., (2010), Energy gaps and a zero-field quantum Hall effect in graphene by strain engineering. *Nature Phys.* 6: 30-33.

[19] Liang G., Neophytou N., Lundstrom M. S., Nikonov D. E., (2007), Ballistic graphene nanoribbon metal-oxide-semiconductor field-effect transistors: A full real-space quantum transport simulation. *J. Appl. Phys.* 102: 054307-054311.

[20] Zhao P., Guo J., (2009), Modeling edge effects in graphene nanoribbon field-effect transistors with real and mode space methods. *J. Appl. Phys.* 105: 034503-03457.

[21] Yousefi R., Shabani M., Arjmandi M., Ghoreishi S. S., (2013), A computational study on electrical characteristics of a novel band-to-band tunneling graphene nanoribbon FET. *Superlatt. Microstruct.*60: 169-178.

[22] Harrison W. A., (1989), Electronic structure and the properties of solids: The physics of the chemical bond. Courier Corporation. (Dover Books on Physics) Paperback – July 1.

[23] Yang L., Anantram M. P., Han J., Lu J. P., (1999), Band-gap change of carbon nanotubes: Effect of small uniaxial and torsional strain. *Phys. Rev. B*. 60: 13874-13881.

[24] Yoon Y., Guo J., (2007), Analysis of strain effects in ballistic carbon nanotube FETs. *IEEE Transact. Electron Dev.* 54: 1280-1287.